

Singularities and qualitative study in LQC

Llibert Aresté Saló,^{1,*} Jaume Amorós,^{1,†} and Jaume de Haro^{1,‡}

¹*Departament de Matemàtica Aplicada, Universitat Politècnica de Catalunya, Diagonal 647, 08028 Barcelona, Spain*

This work contains a detailed analysis of singularities in General Relativity and in Loop Quantum Cosmology, yielding explicit analytical expressions for the energy density and the Hubble parameter for a given set of possible Equations of State. The case when the background is driven by a single scalar field is also considered, obtaining analytical expressions for the corresponding potential. And, in a given particular case, a qualitative study of the orbits in the associated phase space of the scalar field is performed.

Keywords: Cosmic Singularity, Loop Quantum Cosmology, Qualitative Study

1. INTRODUCTION

Soon after Einstein published the field equations of General Relativity (GR) [1], it was realized that these equations contained singularities. In particular, in a cosmological context, it was noticed that for the Friedmann-Lemaître-Robertson-Walker geometry, when the Equation of State (EoS) modeling the matter content was a linear equation with an EoS parameter greater than -1 , a singularity named Big Bang appeared at early times, where the energy density of the universe diverges. Moreover, dealing with nonlinear EoS (see for instance, [2], where the analysis is done by expressing the EoS in the form of a power expansion) one can see that other kind of singularities such as Sudden singularity [3–5] or Big Freeze [6–10] appear.

Several attempts to remove these kinds of singularities were studied for years. We can mention, for instance, the assumption of a non-linear EoS [11] with two points where the pressure plus energy density vanishes leading to two fixed points or the modification of the Friedmann equation assuming that the square of the Hubble parameter is equal to a power series of the energy density [12]. Another option is the introduction of higher order terms in the equations of GR via the quantum effects of a scalar field conformally coupled with gravity [13–17] or directly assuming a Lagrangian containing non-linear terms in the scalar curvature [18–20]. However, the simplest way to remove the Big Bang singularity is to adopt the viewpoint of Loop Quantum Cosmology (LQC), where the discrete nature of spacetime is assumed and the Friedmann equations are modified. Hence, the Big Bang is replaced by a non-singular bounce.

The aim of this paper is to study singularities both in GR and in Loop Quantum Cosmology (LQC) when the universe is filled with a fluid with EoS $P = -\rho - A\rho^\alpha$, since it contains some of the singularities that we have already mentioned. Moreover, we will qualitatively study when we have a scalar field φ which mimicks this fluid. Among the infinite solutions that arise from the conservation equation, which can be plotted in the phase space $(\varphi, \dot{\varphi})$, there is only one -the only one that could be calculated analytically- which gives the same background as the fluid, and what we will study is whether this solution is an attractor or a repeller of the dynamical system that comes from the conservation equation. This study is very important in the so-called matter bounce and matter-ekpyrotic bounce scenario [21–24], because all the calculations -the power spectrum of perturbations, the spectral index, its running [21, 25, 26] and the reheating temperature [27, 28]- are done with the analytical solution, but of course these calculations are only viable if this solution is stable, in the sense that all the other solutions depict asymptotically a universe with the same properties.

The work is organized as follows:

In section 2, we derive the Friedmann equations for a flat homogeneous and isotropic space-time from Einstein's field equation of GR, analyzing its singularities for an EoS $P = -\rho - A\rho^\alpha$, as done in [29]. After the classification of the singularities, we reconstruct the scalar field and the corresponding potential which lead to the same background as the fluid with EoS $P = -\rho - A\rho^\alpha$. Finally, for the case $\alpha = 1$, i.e. for a linear EoS, we perform a qualitative study of the dynamical equations, obtaining the phase portraits for the different values of the effective EoS parameter, and concluding that when the effective EoS parameter belongs to the interval $(-1, 1)$ the analytical orbit is a repeller in the contracting phase and an attractor in the

*Electronic address: llibert.arestes@estudiant.upc.edu

†Electronic address: jaume.amoros@upc.edu

‡Electronic address: jaime.haro@upc.edu

expanding one. On the contrary, when the effective EoS parameter is greater than 1, i.e., in the ekpyrotic case, the analytical orbit is an attractor in the contracting phase and a repeller in the expanding one.

Finally, in section 3, we proceed analogously as with GR, but now including in the Friedmann equations holonomic corrections that come from LQC. Since the equations become more complicated, when analyzing singularities and reconstructing the scalar field, we will not be able to obtain analytical results for every value of α in the EoS, but only for certain particular values, treating some further cases than the ones in [30]. However, we perform a detailed classification of the singularities, both stating which types can be avoided in comparison to GR and which values of α lead to the types that persist. We also verify that the ρ^2 correction origins a bounce, preventing the existence of Big Bang and Big Rip [31] singularities, that will be explained later in a more detailed way. Finally, we do as well a qualitative study for dynamical equations of the scalar field, obtaining similar phase portraits as the one shown in [32] for a particular case of the ones we are going to study in the present work.

We will use natural units ($\hbar = 8\pi G = c = 1$).

2. GENERAL RELATIVITY

2.1. Friedmann Equations

Assuming homogeneity and isotropy of the universe, which is valid at sufficiently large scales, it can be shown that a suitable change of coordinates leads to the so-called Friedmann-Lemaître-Robertson-Walker (FLRW) metric [33]

$$ds^2 = dt^2 - a^2(t) \left(\frac{dr^2}{1 - \kappa r^2} + r^2 d\theta^2 + r^2 \sin^2 \theta d\varphi^2 \right), \quad (1)$$

where $a(t)$ is a scale factor that parametrizes the relative expansion of the universe and the curvature κ is -1, 0 or 1 if we are dealing respectively with an open, flat or closed universe.

To simplify, we will perform all our calculations in the flat FLRW space-time. Hence, with the EoS $P = -\rho - f(\rho)$, we obtain the Friedmann equations [34]

$$H^2 = \frac{\rho}{3}, \quad \dot{H} = \frac{f(\rho)}{2}, \quad \dot{\rho} = 3Hf(\rho), \quad (2)$$

where $H = \frac{\dot{a}}{a}$ is the Hubble parameter.

In next section we will particularize with the EoS given by $f(\rho) = A\rho^\alpha$ [29]. Firstly we analyze the singularities and then we will introduce a scalar field with its corresponding potential. Finally we will qualitatively study the dynamical system for the linear case ($\alpha = 1$).

2.2. Analysis of the singularities

Solving equation (2), we have to distinguish whether we are in the expanding phase ($H = H_+ > 0$) or contracting phase ($H = H_- < 0$)

$$\rho_{\pm}(t) = \begin{cases} \left(\rho_0^{1/2-\alpha} \pm \sqrt{3} \left(\frac{1}{2} - \alpha \right) A t \right)^{1/(1-2\alpha)} & \alpha \neq \frac{1}{2} \\ \rho_0 e^{\pm A \sqrt{3} t} & \alpha = \frac{1}{2}, \end{cases} \quad (3)$$

where ρ_0 is the energy density at $t = 0$.

The case $\alpha = 1/2$, corresponding to $H = H_0 e^{\pm A \sqrt{3} t/2}$ leads, in the expanding phase, to the so-called ‘‘Little Rip’’ singularity [35, 36] for a phantom fluid and a ‘‘Little Bang’’ [29] -there are not singularities at finite cosmic time and the effective EoS parameter tends asymptotically to -1 at early times- for a standard fluid. Thus, we suppose $\alpha \neq \frac{1}{2}$.

$$\begin{cases} H_+(t) = \left(H_0^{1-2\alpha} + \frac{3^\alpha}{2} (1-2\alpha) A t \right)^{1/(1-2\alpha)} \\ H_-(t) = - \left((-H_0)^{1-2\alpha} - \frac{3^\alpha}{2} (1-2\alpha) A t \right)^{1/(1-2\alpha)}. \end{cases} \quad (4)$$

If $A = 0$, $(\rho(t), H(t)) = (\rho_0, H_0)$ and $a(t) = a_0 e^{H_0(t-t_0)}$. Therefore, from now on, we will consider the more interesting case $A \neq 0$. Define $t_s^\pm = \pm \frac{2|H_0|^{1-2\alpha}}{3^\alpha(2\alpha-1)A}$, which for $A < 0$ is positive when $\alpha < 1/2$ and negative when $\alpha > 1/2$ in the expanding phase, and vice-versa in the contracting phase. Then, the Hubble parameter is given by

$$H_\pm(t) = \pm \left(\pm \frac{3^\alpha}{2} (1 - 2\alpha) A (t - t_s^\pm) \right)^{1/(1-2\alpha)} \equiv \pm (k_\pm (t - t_s^\pm))^{1/(1-2\alpha)}, \quad (5)$$

and the scale factor by

$$\begin{cases} \ln \left(\frac{a_\pm(t)}{a_s} \right) = \frac{1}{(1-\alpha) \cdot 3^\alpha A} (k_\pm (t - t_s^\pm))^{2(1-\alpha)/(1-2\alpha)} & \alpha \neq 1 \\ a_\pm(t) = a_s |t - t_s^\pm|^{\pm 1/k_\pm} & \alpha = 1. \end{cases} \quad (6)$$

From these expressions it is rather easy to analyze all the singularities, but first of all, we will classify them in the following types, as done in [6] (see also [37] for a more detailed classification):

FUTURE SINGULARITIES:

- Type I (Big Rip): $t \rightarrow t_s$, $a \rightarrow \infty$, $\rho \rightarrow \infty$ and $|P| \rightarrow \infty$.
- Type II (Sudden): $t \rightarrow t_s$, $a \rightarrow a_s$, $\rho \rightarrow \rho_s$ and $|P| \rightarrow \infty$.
- Type III (Big Freeze): $t \rightarrow t_s$, $a \rightarrow a_s$, $\rho \rightarrow \infty$ and $|P| \rightarrow \infty$.
- Type IV (Generalized Sudden): $t \rightarrow t_s$, $a \rightarrow a_s$, $\rho \rightarrow 0$, $|P| \rightarrow 0$ and derivatives of H diverge.

PAST SINGULARITIES (defined analogously as the future ones, as in [29]):

- Type I (Big Bang): $t \rightarrow t_s$, $a \rightarrow 0$, $\rho \rightarrow \infty$ and $|P| \rightarrow \infty$.
- Type II (Past Sudden): $t \rightarrow t_s$, $a \rightarrow a_s$, $\rho \rightarrow \rho_s$ and $|P| \rightarrow \infty$.
- Type III (Big Hottest): $t \rightarrow t_s$, $a \rightarrow a_s$, $\rho \rightarrow \infty$ and $|P| \rightarrow \infty$.
- Type IV (Generalized past Sudden): $t \rightarrow t_s$, $a \rightarrow a_s$, $\rho \rightarrow 0$, $|P| \rightarrow 0$ and derivatives of H diverge.

According to the different possible values of α , we are going to particularize for the expanding phase and $A < 0$, using equations (5) and (6):

- If $\alpha > 1/2$, H is defined for $t > t_s$ and $t = t_s$ is a past singularity where $H \rightarrow \infty$, $\dot{H} \rightarrow -\infty$ and

$$a \rightarrow \begin{cases} a_s, & \alpha > 1 \\ 0 & \text{(polynomially)}, \quad \alpha = 1 \\ 0 & \text{(exponentially)}, \quad \frac{1}{2} < \alpha < 1. \end{cases} \quad (7)$$

Thus, $\alpha > 1$ corresponds to a Type III singularity, while $\frac{1}{2} < \alpha \leq 1$ is a Type I singularity.

- If $\alpha < 1/2$, H is defined for $t < t_s$ and, in $t \rightarrow t_s$, $H \rightarrow 0$ and, hence, $a \rightarrow a_s$. From $P = -\rho - A\rho^\alpha$, it is trivial to see that, when $t \rightarrow t_s$, for $\alpha < 0$, $P \rightarrow -\infty$ (corresponding to a Type II future singularity). For $\alpha = 0$, when $t \rightarrow t_s$, $\dot{H} = \frac{A\rho^\alpha}{2}$ is constant, and so for this case we have no singularities. Regarding the values $0 < \alpha < 1/2$, we see that, given $k \in \mathbb{N}$, $\frac{d^k H}{dt^k} = C_k \cdot \rho^{\alpha k - \frac{1}{2}(k-1)}$, where C_k is independent on ρ . Then, we can easily verify that when $\rho \rightarrow 0$,

$$\frac{d^k H}{dt^k} \rightarrow \begin{cases} \text{constant,} & \text{if } \alpha = \frac{k-1}{2k} \\ \pm\infty, & \text{if } \alpha < \frac{k-1}{2k} \text{ and } \alpha \neq \frac{r-1}{2r} \\ 0, & \text{otherwise.} \end{cases} \quad \forall r \in \mathbb{N} \quad (8)$$

Hence, in the first and third case there are no singularities, while the second case corresponds to Type IV future singularities.

Finally, we would like to remark that, for the cases not treated, the analysis would be analogous and yield the same types of singularities.

2.3. Reconstruction method

The perfect fluid which fills FLRW space-time could be mimicked by a scalar field defined in all space-time with a kinetic and a potential term. By reconstruction, we mean that we are going to obtain the potential to which this scalar field is submitted as a function of the parameters that define the EoS. For the case $A < 0$, we need a scalar field φ , spatially homogeneous, subject to a potential $V(\varphi)$, such that [38]

$$\rho = \frac{\dot{\varphi}^2}{2} + V(\varphi), \quad P = \frac{\dot{\varphi}^2}{2} - V(\varphi). \quad (9)$$

The conservation equation $\dot{\rho} = -3H(\rho + P) = -3H\dot{\varphi}^2$ leads to

$$\ddot{\varphi} + 3H_{\pm}(\varphi, \dot{\varphi})\dot{\varphi} + V_{\varphi} = 0, \quad (10)$$

where $H_{\pm}(\varphi, \dot{\varphi}) = \pm \frac{1}{\sqrt{3}} \sqrt{\frac{\dot{\varphi}^2}{2} + V(\varphi)}$, with H_+ (resp. H_-) referring to the expanding (resp. contracting) phase.

Now, from equation (5) and Raychaudhuri equation $\dot{H} = -\frac{\rho+P}{2} = -\frac{\dot{\varphi}^2}{2}$, choosing the scalar field φ to be an increasing function, we obtain for $\alpha \neq 1/2$

$$\dot{\varphi}_{\pm}(t) = \sqrt{-3\alpha A} (k_{\pm}(t - t_s^{\pm}))^{\alpha/(1-2\alpha)}. \quad (11)$$

Therefore, when $\alpha \neq 1$ we have

$$\varphi_{\pm}(t) = \varphi_0 \pm \frac{2}{\sqrt{-A3^{\alpha}}} \frac{1}{\alpha - 1} (k_{\pm}(t - t_s^{\pm}))^{(1-\alpha)/(1-2\alpha)} \quad (12)$$

Hence, from this relation between φ and t and using equation (5), we get

$$H_{\pm}(\varphi) = \pm \left(\pm \frac{\sqrt{-A3^{\alpha}}}{2} (\alpha - 1)(\varphi - \varphi_0) \right)^{1/(1-\alpha)}. \quad (13)$$

To compute the potential, we use that $V(\varphi) = \rho - \frac{\dot{\varphi}^2}{2} = \rho + \frac{f(\rho)}{2} = \rho + \frac{A}{2}\rho^{\alpha}$, obtaining

$$V_{\pm}(\varphi) = 3 \left(\pm \frac{\sqrt{-A3^{\alpha}}}{2} (\alpha - 1)(\varphi - \varphi_0) \right)^{2/(1-\alpha)} + \frac{A3^{\alpha}}{2} \left(\pm \frac{\sqrt{-A3^{\alpha}}}{2} (\alpha - 1)(\varphi - \varphi_0) \right)^{2\alpha/(1-\alpha)}. \quad (14)$$

We consider now the case $\alpha = 1$, which corresponds to the Equation of State $P = \omega\rho$, that is $f(\rho) = -(\omega + 1)\rho$. Thus, if $A < 0$ we are considering $\omega > -1$. The scalar field will have the following expression

$$\dot{\varphi}_{\pm}(t) = \frac{2}{\sqrt{3(1+\omega)}} \frac{1}{|t - t_s^{\pm}|}, \quad \varphi_{\pm}(t) = \pm \frac{1}{\sqrt{3(1+\omega)}} \ln \left(\left(\frac{t - t_s^{\pm}}{t_0} \right)^2 \right), \quad (15)$$

and the potential will be such that $(\omega + 1) \left(\frac{\dot{\varphi}^2}{2} + V(\varphi) \right) = \dot{\varphi}^2$. Then, from relation (15), we arrive at

$$V_{\pm}(\varphi) = \frac{1 - \omega}{1 + \omega} \frac{\dot{\varphi}_{\pm}^2}{2} = V_0 e^{\mp \sqrt{3(1+\omega)}\varphi}, \quad (16)$$

where we have taken $t_0^2 = \frac{2(1-\omega)}{3(1+\omega)^2 V_0}$.

Finally, we will analyze the case $\alpha = 1/2$. From the expression obtained in equation (4), we see that there is a Little Bang singularity. In this case the scalar field turns out to be

$$\dot{\varphi}_{\pm}(t) = \sqrt{-\sqrt{3}A|H_0|} e^{\pm \frac{\sqrt{3}}{4}At}, \quad \varphi_{\pm}(t) = \varphi_0 \pm 4 \frac{\sqrt{-\sqrt{3}A|H_0|}}{\sqrt{3}A} e^{\pm \frac{\sqrt{3}}{4}At}. \quad (17)$$

From this relation and using the case $\alpha = 1/2$ in equation (3), we obtain

$$V(\varphi) = \frac{-3A^2}{32} (\varphi - \varphi_0)^2 \left(1 - \frac{3}{8} (\varphi - \varphi_0)^2 \right). \quad (18)$$

Regarding the case $A > 0$, all the results are very similar. The only difference is that we need to consider a phantom scalar field, i.e, such that $\rho = -\frac{\dot{\varphi}^2}{2} + V(\varphi)$ and $P = -\frac{\dot{\varphi}^2}{2} - V(\varphi)$.

2.4. Dynamics for the linear case

In the case of the linear EoS $P = \omega\rho$ with $\omega > -1$, we want to study the behavior of the analytical solution, finding out if it is either an attractor or a repeller [39] and comparing its behavior with that of other solutions of the system. We will analyze the dynamics in the contracting phase from this dynamical system

$$\ddot{\varphi} + 3H_-(\varphi, \dot{\varphi}) + V_\varphi = 0, \quad (19)$$

where $H_-(\varphi, \dot{\varphi}) = -\sqrt{\frac{\dot{\varphi}^2}{2} + V(\varphi)}$ and $V(\varphi) = V_0 e^{\sqrt{3(1+\omega)}\varphi}$.

With the change of variable $\varphi = \frac{-2}{\sqrt{3(1+\omega)}} \ln \psi$, the dynamical system becomes

$$\frac{d\dot{\psi}}{d\varphi} = F_-(\dot{\psi}) := -\frac{3}{2}\sqrt{1+\omega} \left(\sqrt{\frac{2\dot{\psi}^2}{3(1+\omega)} + V_0} + \frac{\sqrt{3}(1+\omega)}{2\dot{\psi}} \left(\frac{2\dot{\psi}^2}{3(1+\omega)} + V_0 \right) \right). \quad (20)$$

The different cases to distinguish are the following ones:

- $\omega = 1$: This case is known as a kination (or deflationary) phase [40, 41]. Equation (20) becomes $\frac{d\dot{\psi}}{d\varphi} = -\sqrt{\frac{3}{2}}(|\dot{\psi}| + \dot{\psi})$, and in the semi-plane $\dot{\psi} \geq 0$ ($\dot{\psi} \leq 0$), the solution is given by

$$(\varphi(t), \dot{\varphi}(t)) = \left(-\sqrt{\frac{2}{3}} \ln(-|C|(t - t_s)), -\sqrt{\frac{2}{3}} \frac{1}{t - t_s} \right) \quad \text{with } t < t_s, \quad (21)$$

which is a stable orbit coinciding with the result obtained in equation (15), with the sign corresponding to the contracting phase. Therefore, this solution corresponds all the time to a universe with EoS $P = \omega\rho$ in the contracting phase, with $H(t) = \frac{1}{3(t-t_s)}$.

Regarding the semi-plane $\dot{\psi} > 0$ ($\dot{\varphi} < 0$), the solution becomes

$$(\varphi(t), \dot{\varphi}(t)) = \left(\sqrt{\frac{2}{3}} \ln(-|C|(t - t_s)), \sqrt{\frac{2}{3}} \frac{1}{t - t_s} \right) \quad \text{with } t < t_s, \quad (22)$$

which is stable analogously to the former case.

Finally, the case $\dot{\psi} = 0$, i.e. $(\varphi(t), \dot{\varphi}(t)) = (C, 0)$, corresponds to $H = 0$.

- $-1 < \omega < 1$: Given that $F_-(\dot{\psi})$ can only vanish for $\dot{\psi} < 0$, we have a single critical point for $\dot{\psi}$

$$\dot{\psi}_- = -(1+\omega) \sqrt{\frac{3V_0}{2(1-\omega)}}, \quad (23)$$

which is a global repeller, given that $F_-(\dot{\psi}) > 0 \quad \forall \dot{\psi}_- < \dot{\psi} < 0$ and $F_-(\dot{\psi}) < 0 \quad \forall \dot{\psi} < \dot{\psi}_-$.

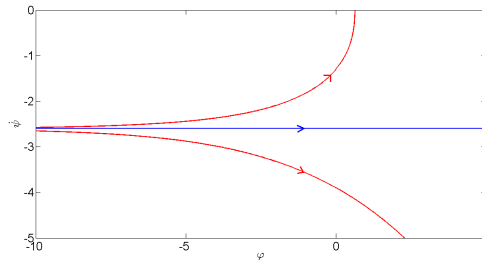


Figure 1: Phase portrait for $\omega = 1/2$ and $V_0 = 1$.

We point out that the blue horizontal line in Figure 1 coincides with equation (15), depicting a universe with EoS $P = \omega\rho$.

- $\omega > 1$: This case is known as an ekpyrotic phase or regime [42] and the system is only defined for $|\dot{\psi}| \geq \sqrt{\frac{3(1+\omega)|V_0|}{2}}$. We have three critical points

$$\dot{\psi}_- = -(1+\omega)\sqrt{\frac{3|V_0|}{2|1-\omega|}}, \quad \dot{\psi}_0^\pm = \pm\sqrt{\frac{3(1+\omega)|V_0|}{2}}, \quad (24)$$

where $\dot{\psi}_0^\pm$ are repellers corresponding to $H = 0$. On the other hand, $\dot{\psi}_-$ is an attractor for $\dot{\psi} < \dot{\psi}_0^-$, solution that leads to a universe that all the time behaves as $P = \omega\rho$ in the contracting phase.

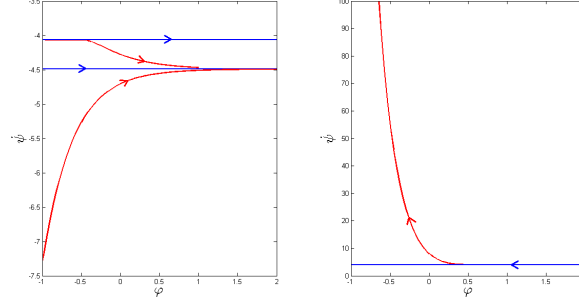


Figure 2: Phase portrait for $\omega = 10$ and $V_0 = -1$.

In the plot on the left-hand side, the upper horizontal line represents $\dot{\psi}_0^-$, corresponding to $H = 0$, while the lower horizontal line is the analytical solution. On the right, for the semiplane $\dot{\psi} > 0$, the blue horizontal line is $\dot{\psi}_0^+$, which corresponds to $H = 0$. In both plots, we appreciate that the orbits behave as expected.

An analogous analysis for the expanding phase [39] would show that for $\omega = 1$ there are as well solutions coinciding with (15) and others with $H = 0$. The solution that depicts a fluid with EoS $P = \omega\rho$ is an attractor for $|\omega| < 1$ and a repeller for $\omega > 1$, also coinciding with equation (15). And for $\omega > 1$, we would also find critical points corresponding to $H = 0$, as the ones found in the contracting phase, that are in this case attractors.

3. LOOP QUANTUM COSMOLOGY

3.1. Modified Friedmann equations

The general formula of loop gravity, which takes into account the discrete nature of space-time, expresses the Hamiltonian in terms of the holonomies $h_j(\lambda) \equiv e^{-i\frac{\lambda\beta}{2}\sigma_j}$, where σ_j are the Pauli matrices [30, 43]

$$\mathcal{H}_{\text{LQC}} = -\frac{2V}{\gamma^3\lambda^3} \sum_{i,j,k} \epsilon^{ijk} \text{Tr}[h_i(\lambda)h_j(\lambda)h_i^{-1}(\lambda)h_j^{-1}(\lambda)\{h_k^{-1}(\lambda), V\}] + \rho V, \quad (25)$$

where $\gamma \approx 0.2375$ is the Barbero-Immirzi parameter and $\lambda = \sqrt{\frac{\sqrt{3}}{4}}\gamma$ is a parameter with the dimension of length, which is determined by invoking the quantum nature of the geometry.

The Hamiltonian expression in (25) leads to [44, 45]

$$\mathcal{H}_{\text{LQC}} = -3V \frac{\sin^2(\lambda\beta)}{\gamma^2\lambda^2} + \rho V. \quad (26)$$

Then, using Hamiltonian equation $\dot{V} = \{V, \mathcal{H}_{\text{LQC}}\} = -\frac{\gamma}{2} \frac{\partial \mathcal{H}_{\text{LQC}}}{\partial \beta}$ and imposing the Hamiltonian constraint $\mathcal{H}_{\text{LQC}} = 0$, i.e., $\rho = \frac{3\sin^2(\lambda\beta)}{\gamma^2\lambda^2}$, we obtain

$$H^2 = \frac{\sin^2(2\lambda\beta)}{4\gamma^2\lambda^2} = \frac{\sin^2(\lambda\beta)}{\gamma^2\lambda^2} (1 - \sin^2(\lambda\beta)) = \frac{\rho}{3} \left(1 - \frac{\rho}{\rho_c}\right), \quad (27)$$

where $\rho_c = \frac{3}{\gamma^2 \lambda^2}$ is the so-called critical energy density (the maximum value that reaches the energy density).

Equation (27) corresponds to an ellipse in the plane (ρ, H) , that we can parametrize in the following form

$$\begin{cases} H = \sqrt{\frac{\rho_c}{12}} \sin \eta \\ \rho = \rho_c \cos^2 \frac{\eta}{2}. \end{cases} \quad (28)$$

The conservation equation does not differ from standard GR, i.e., the fluid fulfills the relation $d(\rho V) = -P dV$, where $V = a^3$, and again with the EoS $P = -\rho - f(\rho)$, one gets $\dot{\rho} = 3H f(\rho)$. Hence, we easily obtain the Raychadhuri equation

$$\dot{H} = \frac{f(\rho)}{2} \left(1 - \frac{2\rho}{\rho_c} \right).$$

From the conservation equation with the parametrization proposed in (28), it is straightforward to obtain the following relation between the parameter η and the cosmic time

$$\int_{\eta_0}^{\eta} \frac{dx}{\cos^{2\alpha} \frac{x}{2}} = -A\sqrt{3}\rho_c^{\alpha-\frac{1}{2}} t \equiv \theta t, \quad (29)$$

with $\eta_0 = \arcsin \left(H_0 \sqrt{\frac{12}{\rho_c}} \right)$, where in the expansive phase $0 < \eta_0 < \pi$, while in the contracting one $\pi < \eta_0 < 2\pi$.

Therefore, in the cases that it was possible to solve analytically this integral one will obtain an analytic expression of the evolution of the universe. We will see some examples in next subsection.

3.2. Analysis of the singularities

In LQC, one never finds singularities of Type I and III because the ellipse is a bounded subset, meaning that the energy density and the Hubble parameter are always finite quantities. Thus, the only singularities that we can find in LQC are for finite ρ and H . For our case, i.e. $f(\rho) = A\rho^\alpha$, we find:

- Type II singularity: It appears for $\alpha < 0$, since in this case $|P| \rightarrow \infty$ when $\rho \rightarrow 0$.
- Type IV singularity: They can be found with the same analysis that was done in Einstein cosmology, since the behaviour of modified Friedmann Equation near $\rho = 0$ is asymptotically the same as without the holonomic correction. Hence, near $\rho = 0$ it is satisfied that $\frac{d^k H}{dt^k} = C_k \cdot \rho^{\alpha k - \frac{1}{2}(k-1)}$, where C_k is independent on ρ . Therefore, for values $0 < \alpha < 1/2$ such that $\alpha \neq \frac{r-1}{2r} \forall r \in \mathbb{N}$, there exists $m \in \mathbb{N}$ for which $\frac{d^m H}{dt^m}$ diverges when $\rho \rightarrow 0$, being therefore Type IV singularities.

Analyzing the dynamical system coming from Friedmann and Raychaudhuri equations

$$\begin{cases} \dot{\rho} = 3H A \rho^\alpha \\ \dot{H} = \frac{A \rho^\alpha}{2} \left(1 - \frac{2\rho}{\rho_c} \right), \end{cases} \quad (30)$$

we see that for $\alpha > 0$ the point $(0, 0)$ will be a fixed point, concretely a saddle point. We observe that the dynamical system is not \mathcal{C}^k for $\alpha < k$, with $k \in \mathbb{N}$. We will consider that $A \neq 0$, which corresponds as in GR to $(\rho(t), H(t)) = (\rho_0, H_0)$ and $a(t) = a_0 e^{H_0(t-t_0)}$. In the plane (ρ, H) , the evolution in the ellipse determined by equation (30) will be anti-clockwise for $A < 0$ (non-phantom fluid) and clockwise for $A > 0$ (phantom fluid). We see, as well, that the time spent to do a complete round in the ellipse starting from $(0, 0)$ is

$$t = 2 \int_0^{\rho_c} \frac{d\rho}{\sqrt{3\rho} \sqrt{1 - \frac{\rho}{\rho_c}} |A| \rho^\alpha}, \quad (31)$$

which diverges for $\alpha \geq 1/2$.

We also point out that in all cases there will be a bounce, since the time that the universe lasts to bounce when it has a energy density $\rho_0 \neq 0$ is $\int_{\rho_0}^{\rho_c} \frac{d\rho}{\sqrt{3\rho} \sqrt{1 - \frac{\rho}{\rho_c}} |A| \rho^\alpha}$, which converges $\forall \alpha$.

Now we can proceed to analyze some values of α , in all cases solving equation (29) and using the parametrization in (28) to find the expressions of $H(t)$ and $\rho(t)$, so as to finally compute $a(t)$ from $H = \frac{\dot{a}}{a}$.

- $\alpha = 1$: It corresponds to the linear EoS $P = \omega\rho$ [39]. So, $2 \tan \frac{\eta}{2} = \theta(t - t_0)$, where $t_0 = -\frac{2}{\theta} \tan \frac{\eta_0}{2}$ is the bouncing time. Therefore, the relevant quantities are given by

$$H(t) = \frac{1+\omega}{2} \frac{\rho_c(t-t_0)}{\frac{3}{4}(1+\omega)^2 \rho_c(t-t_0)^2 + 1}, \quad \rho(t) = \frac{\rho_c}{\frac{3}{4}(1+\omega)^2 \rho_c(t-t_0)^2 + 1}, \quad (32)$$

$$a(t) = a_0 \left(1 + \frac{3}{4}(1+\omega)^2 \rho_c(t-t_0)^2\right)^{\frac{1}{3(1+\omega)}}.$$

- $\alpha = 0$:

$$H(t) = \sqrt{\frac{\rho_c}{12}} \sin(\theta(t-t_0)), \quad \rho(t) = \rho_c \cos^2\left(\frac{\theta}{2}(t-t_0)\right), \quad \ln \frac{a(t)}{a_0} = -\sqrt{\frac{\rho_c}{12}} \frac{1}{\theta} (\cos(\theta(t-t_0)) - 1), \quad (33)$$

where $t_0 = -\frac{\eta_0}{\theta}$ is the bouncing time.

- $\alpha = \frac{1}{2}$: Solving equation (29), we have that $2 \ln \left(\tan \frac{\eta}{2} + \sec \frac{\eta}{2}\right) = \theta(t-t_0)$, where $t_0 = -\frac{2}{\theta} \ln \left(\tan \frac{\eta_0}{2} + \sec \frac{\eta_0}{2}\right)$ is the bouncing time. Hence, $\cos \frac{\eta}{2} = \cosh^{-1} \left(\frac{\theta(t-t_0)}{2}\right)$ and

$$H(t) = -\sqrt{\frac{\rho_c}{3}} \frac{\sinh \frac{\theta(t-t_0)}{2}}{\cosh^2 \frac{\theta(t-t_0)}{2}}, \quad \rho(t) = \frac{\rho_c}{\cosh^2 \frac{\theta(t-t_0)}{2}}, \quad \ln \frac{a(t)}{a_0} = -\frac{2\sqrt{3}\rho_c}{3\theta} \left(\frac{1}{\cosh \frac{\theta(t-t_0)}{2}} - 1\right). \quad (34)$$

- $\alpha = -\frac{1}{2}$: In this case we obtain the following expressions

$$H(t) = \sqrt{\frac{\rho_c}{12}} \theta(t-t_0) \sqrt{1 - \frac{\theta^2(t-t_0)^2}{4}}, \quad \rho(t) = \rho_c \left(1 - \frac{\theta^2(t-t_0)^2}{4}\right), \quad (35)$$

$$\ln \frac{a(t)}{a_0} = \frac{2\sqrt{3}\rho_c}{9} \left[1 - \left(1 - \frac{\theta^2(t-t_0)^2}{4}\right)^{3/2}\right],$$

defined for $|t-t_0| \leq \frac{2\rho_c}{|A|\sqrt{3}}$, where $t_0 = -\frac{2}{\theta} \cos \frac{\eta_0}{2}$ is the bouncing time. And we have a Type II singularity at $t_s^\pm = t_0 \pm \frac{2\rho_c}{A\sqrt{3}}$.

3.3. Reconstruction method

Now we will proceed, as done with General Relativity, to build the potential from the scalar field φ . We will work in the case $A < 0$ (non-phantom), so the scalar field will satisfy relations in (9). We analyze separately the different cases:

- $\alpha = 1$: It corresponds to the linear EoS $P = \omega\rho$, with $\omega > -1$. Thus, reminding (9), we obtain

$$\dot{\varphi}^2 = \frac{(1+\omega)\rho_c}{\frac{3}{4}(1+\omega)^2 \rho_c(t-t_0)^2 + 1}, \quad (36)$$

and

$$\varphi(t) = \frac{2}{\sqrt{3(1+\omega)}} \ln \left(\frac{\frac{\sqrt{3\rho_c}}{2}(1+\omega)(t-t_0) + \sqrt{\frac{3\rho_c}{4}(1+\omega)^2 \rho_c(t-t_0)^2 + 1}}{|\tilde{\varphi}_0|} \right), \quad (37)$$

where $\varphi_0 = -\frac{2}{\sqrt{3(1+\omega)}} \ln |\tilde{\varphi}_0|$.

So, now we can compute the potential as a function of the scalar field. Taking $\tilde{\varphi}_0^2 = \frac{V_0}{2\rho_c(1-\omega)}$ and using equation (37), it is easy to check

$$V(\varphi) = V_0 \frac{e^{\sqrt{3(1+\omega)}\varphi}}{\left(1 + \frac{V_0}{2\rho_c(1-\omega)} e^{\sqrt{3(1+\omega)}\varphi}\right)^2}. \quad (38)$$

- $\alpha = 0$: In this case the scalar field is $\varphi(t) = \varphi_0 + \sqrt{-A}(t - t_0)$. Thus, using (33), the corresponding potential is

$$V(\varphi) = \rho_c \cos^2 \left(\sqrt{\frac{-3A}{\rho_c}} \frac{\varphi - \varphi_0}{2} \right) + \frac{A}{2}. \quad (39)$$

Regarding the two cases left, it is not possible to integrate analytically the scalar field φ . However, we can express the potential in the following form:

- $\alpha = \frac{1}{2}$: From equation (34), $V = \rho + \frac{A\rho^{1/2}}{2} = \dot{\varphi}^2 \left(\frac{\dot{\varphi}^2}{A^2} - \frac{1}{2} \right)$, where $\dot{\varphi}^2 = -A\rho^{1/2} = -\frac{A\rho_c^{1/2}}{\cosh\left(\frac{\theta(t-t_0)}{2}\right)}$.
- $\alpha = -\frac{1}{2}$: From equation (35), $V = \rho + \frac{A\rho^{1/2}}{2} = \frac{A^2}{\dot{\varphi}^4} - \frac{\dot{\varphi}^2}{2}$, where $\dot{\varphi}^2 = -A\rho^{-1/2} = -\frac{A}{\rho_c^{1/2}\sqrt{1-\frac{\theta^2(t-t_0)^2}{4}}}$.

3.4. Dynamics for the linear case

We want to analyze the behaviour of the solution corresponding to the EoS $P = \omega\rho$ with $\omega > -1$. Using the potential found in (38), we will study the dynamics of the equation

$$\ddot{\varphi} + 3H_{\pm}(\varphi, \dot{\varphi})\dot{\varphi} + V_{\varphi} = 0, \quad (40)$$

where $H_{\pm}(\varphi, \dot{\varphi}) = \pm \sqrt{\frac{\rho(\varphi, \dot{\varphi})}{3} \left(1 - \frac{\rho(\varphi, \dot{\varphi})}{\rho_c} \right)}$, with $\rho(\varphi, \dot{\varphi}) = \frac{\dot{\varphi}^2}{2} + V(\varphi)$.

Firstly, we note that this implies that

$$\dot{\rho} = -3H_{\pm}(\varphi, \dot{\varphi})\dot{\varphi}^2. \quad (41)$$

Therefore, the evolution in time will take place in an anti-clockwise sense throughout the ellipse, being $(0, 0)$ a fixed point.

Before proceeding to the analysis of the different cases, we are going to take a glance at the geometry of the phase space $(\varphi, \dot{\varphi})$.

Since we are dealing with a bi-valued dynamical system, we need a cover 2:1 (of two sheets) of the allowed region in the plane of the phase space $(\varphi, \dot{\varphi})$, which is ramified in the curves $H(\varphi, \dot{\varphi}) = 0$. Hence, for the case $|\omega| < 1$, this is a cylinder, whereas for $\omega > 1$ we have two cylinders, as we can see in Figure 3. This explains why in the phase portrait that we will later obtain we can have intersecting orbits, which happens always between an orbit in the expanding phase and another one in the contracting phase.

Therefore, when solving the dynamical system one option would be to use local coordinates in a cylinder. However, this would be cumbersome and, thus, we have opted for integrating the solution taking into account whether we are in the expanding or contracting phase, so that we change sign of H when reaching the curve $H = 0$. For the numerical results, we will use an RK78 method, that holds in memory the sign of H and changes it when we switch from the contracting to the expanding phase.

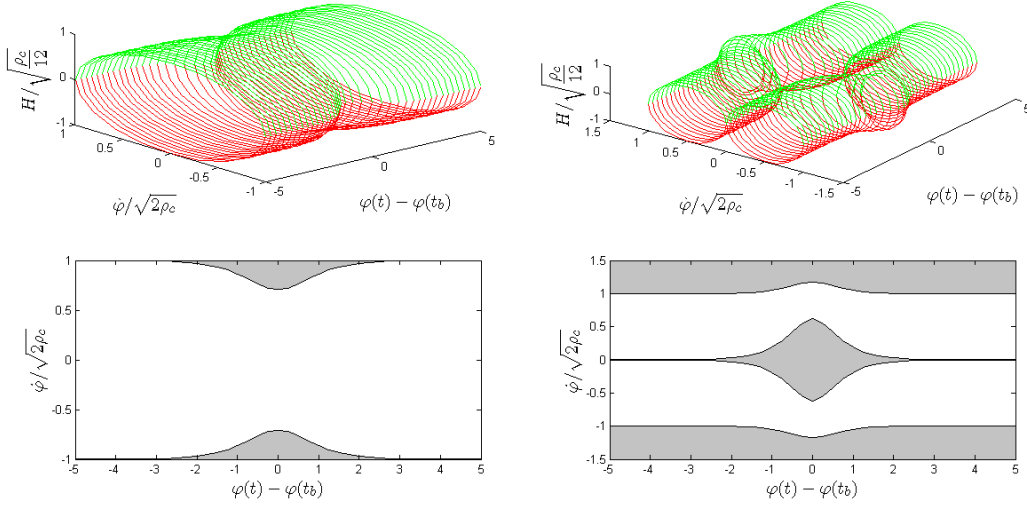


Figure 3: Top row: the phase space $(\varphi, \dot{\varphi}, H)$ for $|\omega| < 1$ (left) and $|\omega| > 1$ (right). The green (resp. red) lines recover all the region corresponding to the expanding (resp. contracting) phase. Bottom row: its projection in the plane $(\varphi, \dot{\varphi})$, in which the white region delimited by the curves $H(\varphi, \dot{\varphi}) = 0$ is the allowed one.

Now, we treat separately the following cases:

- $\omega = 1$: In this case, the potential is zero. Thus, (40) becomes $\ddot{\varphi} = \mp \sqrt{\frac{3}{2}} |\dot{\varphi}| \dot{\varphi} \sqrt{1 - \frac{\dot{\varphi}^2}{2\rho_c}}$.

Since $\rho \leq \rho_c$, $|\dot{\varphi}| \leq \sqrt{2\rho_c}$. Therefore, we can use the change of variables $\dot{\varphi} = \sqrt{2\rho_c} \cos(\xi)$. Assuming that at $t=0$ we are in the expanding phase of the semi-plane $\dot{\varphi}_0 > 0$, we will have $\tan \xi - \tan \xi_0 = \sqrt{3\rho_c} t$. Hence,

$$\dot{\varphi}(t) = \sqrt{\frac{2\rho_c}{1 + (\sqrt{3\rho_c} t + C)^2}}, \quad \text{for } t > \frac{-C}{\sqrt{3\rho_c}}, \quad (42)$$

where $C = \sqrt{\frac{2\rho_c}{\dot{\varphi}_0^2} - 1}$.

It is easy to see that in the contracting phase ($t < \frac{-C}{\sqrt{3\rho_c}}$), the expression of $\dot{\varphi}(t)$ would be exactly analogous. Moreover, if $t=0$ takes place during the contracting phase, the constant C would be defined as $C = -\sqrt{\frac{2\rho_c}{\dot{\varphi}_0^2} - 1}$. Therefore, the orbit in the phase portrait is

$$(\varphi(t), \dot{\varphi}(t)) = \left(\varphi_0 + \sqrt{\frac{2}{3}} \ln \left(\sqrt{3\rho_c} t + C + \sqrt{1 + (\sqrt{3\rho_c} t + C)^2} \right), \sqrt{\frac{2\rho_c}{1 + (\sqrt{3\rho_c} t + C)^2}} \right), \quad (43)$$

and, in the semi-plane $\dot{\varphi}_0 < 0$, it is given by

$$(\varphi(t), \dot{\varphi}(t)) = \left(\varphi_0 - \sqrt{\frac{2}{3}} \ln \left(\sqrt{3\rho_c} t + C + \sqrt{1 + (\sqrt{3\rho_c} t + C)^2} \right), -\sqrt{\frac{2\rho_c}{1 + (\sqrt{3\rho_c} t + C)^2}} \right). \quad (44)$$

Hence, we see that all these are stable orbits that foliate all the space $0 < |\dot{\varphi}| \leq \sqrt{2\rho_c}$, corresponding to the analytical solution found in (37), with the bounce taking place in $t_b = -\frac{C}{\sqrt{3\rho_c}}$ and such that $H(t) = (t - t_b)\rho(t) = \frac{\rho_c(t - t_b)}{1 + 3\rho_c(t - t_b)^2}$.

On the other hand, if $\dot{\varphi}_0 = 0$, the correspondent orbit $(\varphi, \dot{\varphi}) = (\varphi_0, 0)$ would correspond to $\rho(t) = H(t) = 0$.

Before analyzing the other cases, we will introduce the following change of variables, motivated by the solution (37)

$$\psi = \sinh \left(\frac{\varphi \sqrt{3(1 + \omega)}}{2} + \frac{1}{2} \ln \left(\frac{V_0}{2\rho_c(1 - \omega)} \right) \right), \quad (45)$$

where we have taken, as we already did previously, $|\tilde{\varphi}_0|^2 = \frac{V_0}{2\rho_c(1-\omega)}$.

Using the potential found in (38), equation (40) becomes

$$\ddot{\psi} = -3H_{\pm}(\psi, \dot{\psi})\dot{\psi} + \rho(\psi, \dot{\psi})\psi \frac{3(1+\omega)}{2}, \quad (46)$$

where $H_{\pm}(\psi, \dot{\psi}) = \pm \sqrt{\frac{\rho(\psi, \dot{\psi})}{3}} \left(1 - \frac{\rho(\psi, \dot{\psi})}{\rho_c}\right)$ and $\rho = \frac{2}{3(1+\omega)(1+\psi^2)} \left(\dot{\psi}^2 + \frac{3(1-\omega^2)}{4}\rho_c\right)$.

Thus, in order to analyze this dynamical system, we compute the conditions needed for $\ddot{\psi}$ to vanish. They are

$$\rho = 0 \quad \text{or} \quad \left\{ \text{sgn}(H\dot{\psi}) = \text{sgn}(\psi) \text{ and } \left(|\dot{\psi}| = \frac{\sqrt{3\rho_c}}{2}(1+\omega) \text{ or } \psi^2 = \frac{4}{3\rho_c(1-\omega^2)}\dot{\psi}^2 \right) \right\}. \quad (47)$$

Now we can proceed to analyze the rest of cases that are left:

- $|\omega| < 1$: We can distinguish two types of orbits: those that cross the axis $\psi = 0$ (Type I) and those that cross the axis $\dot{\psi} = 0$ (Type II).

Regarding Type I orbits, we are going to consider that at the initial point $t = 0$ we are at $(\psi, \dot{\psi}) = (0, \dot{\psi}_0)$, where $0 < \dot{\psi}_0 \leq \frac{\sqrt{3\rho_c}}{2}(1+\omega)$, which comes from the restriction $0 < \rho_0 \leq \rho_c$. If $\rho_0 = \rho_c$, at $t=0$ we are at the bounce and, by (47), the value of $\dot{\psi}$ will be the same throughout all the contracting and expanding phase, coinciding with the analytical solution found in (37). With respect to Type II orbits, the initial point $t = 0$ will be at $(\psi, \dot{\psi}) = (\psi_0, 0)$ where $\psi_0 \neq 0$. The corresponding phase portrait is given in figure 4 where we have represented the set $\rho = \rho_c$, which is the discontinuous black line corresponding to $\dot{\psi} = \pm \sqrt{\frac{3\rho_c}{2}(1+\omega)(\psi^2 + \frac{1+\omega}{2})}$. The pointed diagonal lines refer to the set where $\ddot{\psi} = 0$, as seen in (47). The blue horizontal lines are the orbits corresponding to the analytical solution.

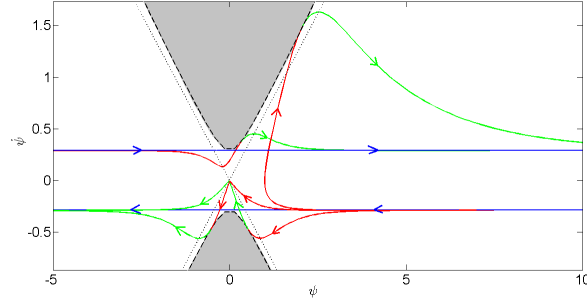


Figure 4: Phase portrait for $w = -2/3$ and $\rho_c = 1$.

With respect to the rest of the curves, we have used the following color notation: red for the contracting phase and green for the expanding phase. We have plotted one possible Type I orbit and one possible Type II orbit. In both we have considered that either $\dot{\psi}_0$ or ψ_0 are in the positive axis and that $t = 0$ takes place during the contracting phase. We note that applying the symmetry with respect to the axis $\dot{\psi} = 0$ and/or $\psi = 0$ we would obtain the other possibilities for these orbits, considering that the initial point is in the negative axis and/or $t = 0$ takes place during the expanding phase.

Finally, in Fig 4 we have drawn as well the invariant curves that come in and out from the saddle point (0,0), the only critical point of the dynamical system. For clarity, we have only plotted the invariant curves for $\dot{\psi} < 0$. The others could be obtained with the symmetry respect to the axis $\dot{\psi} = 0$.

So, we clearly see in each orbit the bounce at the time in which it touches the curve $\rho = \rho_c$. We observe that $\rho = 0$ takes place for $\psi \rightarrow \infty$. The points in which the orbits intersect with the diagonal lines are where they change the sign of their

slope. And finally the horizontal lines corresponding to the analytical solution are attractors for the expanding phase and repellers for the contracting phase.

We can also characterize orbits with the following value:

$$\omega_{\text{eff}}(t) := \frac{P(t)}{\rho(t)} = \frac{\dot{\psi}(t)^2 - \frac{3}{4}(1 - \omega^2)\rho_c}{\dot{\psi}(t)^2 + \frac{3}{4}(1 - \omega^2)\rho_c}. \quad (48)$$

We observe that $-1 \leq \omega_{\text{eff}}(t) < 1$ and that for the analytical value $|\dot{\psi}| = \frac{\sqrt{3\rho_c}}{2}(1 + \omega)$, $\omega_{\text{eff}}(t) = \omega$. Regarding the other orbits, the bounce takes place at $\omega_{\text{eff}}(t_b) > \omega$ and, when $\rho(t) \rightarrow 0$, since all the orbits converges to the analytic one, it can be easily verified that $\omega_{\text{eff}}(t) \rightarrow \omega$.

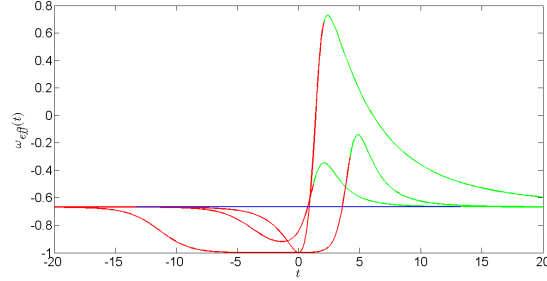


Figure 5: Evolution of $\omega_{\text{eff}}(t)$ for the orbits represented in the phase portrait for $\omega = -2/3$ and $\rho_c = 1$.

- $\omega > 1$: In this case, since the potential is negative, we have the lower bound of $|\dot{\psi}| \geq \frac{\sqrt{3\rho_c}}{2}\sqrt{\omega^2 - 1}$. Therefore, we only have Type I orbits.

If $\rho_0 = 0$, we are stuck in this value of ρ during all the orbit $|\dot{\psi}| = \frac{\sqrt{3\rho_c}}{2}\sqrt{\omega^2 - 1}$. If $\rho_0 = \rho_c$, analogously as in the $|\omega| < 1$ case, we stay throughout all the contracting and expanding phase in the analytical solution. In the phase portrait we have represented as a discontinuous black line the curve corresponding to $\rho = \rho_c$. The other two discontinuous horizontal lines that delimit the forbidden region refer to an orbit with $\rho = 0$. The blue horizontal lines correspond to the orbits coming from the analytical solution.

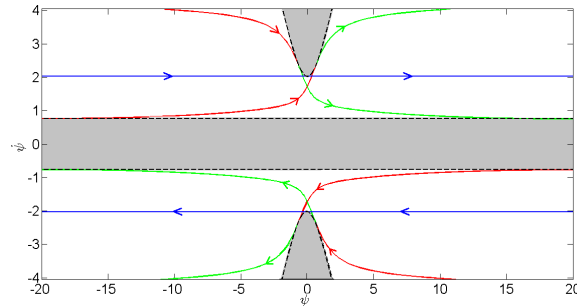


Figure 6: Phase portrait for $w = 4/3$ and $\rho_c = 1$.

Regarding the other orbits, we have used the same colour notation as before. It is important to note that, since $\omega > 1$, the condition $\psi^2 = \frac{4}{3\rho_c(1-\omega^2)}\dot{\psi}^2$ is never fulfilled. Hence, equation (47) implies that the sign of the slope of the orbit can never change, i.e., ψ will always be convex or concave. So, we see that the curve reaches $\rho = 0$ at $\psi \rightarrow \pm\infty$ with $\dot{\psi}$ either converging to $\pm \frac{\sqrt{3\rho_c}}{2}\sqrt{\omega^2 - 1}$ or diverging such that $\frac{\dot{\psi}}{\psi} \rightarrow 0$. We also observe a bounce for $\rho = \rho_c$. Thus, the analytical solution is a repeller in the expanding phase and an attractor (though not global) in the contracting phase.

In this case, the same equation (48) is valid. We observe that $\omega_{eff} > 1$ and that $\omega_{eff} = \omega$ for the analytical orbit. In the other orbits, the bounce takes place at $\omega_{eff}(t_b) < \omega$ and, when $\rho(t) \rightarrow 0$, it is verified that $\omega_{eff}(t) \rightarrow \infty$ when the orbits converge to $\pm \frac{\sqrt{3\rho_c}}{2} \sqrt{\omega^2 - 1}$ or $\omega_{eff}(t) \rightarrow 1$ when $|\dot{\psi}| \rightarrow \infty$.

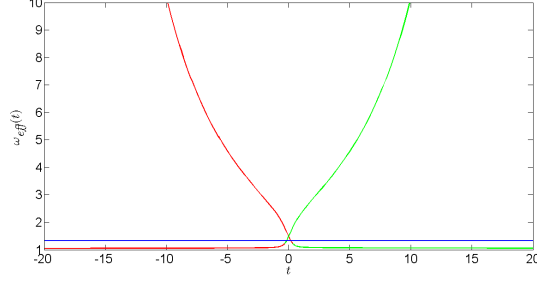


Figure 7: Evolution of $\omega_{eff}(t)$ for the orbits represented in the phase portrait for $w = 4/3$ and $\rho_c = 1$.

In figure 7, we clearly appreciate the two types of orbits:

- Type A: During the beginning of the contracting phase the orbit comes asymptotically from $|\dot{\psi}| = \frac{\sqrt{3\rho_c}}{2} \sqrt{\omega^2 - 1}$ ($\omega_{eff} \rightarrow \infty$), in such a way that the value of $|\dot{\psi}|$ is below the one of the orbit of the analytic solution. Then, it crosses this orbit, bounces and in the expanding phase $|\dot{\psi}| \rightarrow \infty$, i.e. $\omega_{eff} \rightarrow 1$.
- Type B: During the contracting phase the orbit comes asymptotically from $|\dot{\psi}| \rightarrow \infty$ ($\omega_{eff} \rightarrow 1$), so that the value of $|\dot{\psi}|$ is above the one of the orbit of the analytic solution. Then it bounces, crosses this orbit, and in the expanding phase $|\dot{\psi}| \rightarrow \frac{\sqrt{3\rho_c}}{2} \sqrt{\omega^2 - 1}$, i.e. $\omega_{eff} \rightarrow \infty$.

4. CONCLUSIONS

We have explored singularities in General Relativity and in Loop Quantum Cosmology when the Equation of State was given by $P = -\rho - A\rho^\alpha$. We have observed that in LQC we only have Type II and Type IV singularities and, in particular, for $\alpha \geq 1/2$ there are no singularities. Unlike in GR, dealing with LQC we have only been able to calculate analytically $H(t)$ and $\rho(t)$ for certain values of α .

We have introduced as well a scalar field φ that accounts for the perfect fluid that fills the space-time. We have computed its corresponding potential $V(\varphi)$ both in GR and for some values of α in LQC. Moreover, we have observed that for $A < 0$ in the Equation of State, we need a canonical scalar field, while for $A > 0$ it must be a so-called phantom scalar field.

Finally, for the linear EoS (i.e., $\alpha = 1$), we have made both in GR and in LQC a qualitative study of the orbits in the phase space $(\varphi, \dot{\varphi})$, concluding that, for a canonical scalar field (i.e., $\omega > -1$), in the expanding (resp. contracting) phase, the analytical solution is an attractor (resp. repeller) for $|\omega| < 1$ both in GR and LQC. For $\omega > 1$, both in GR and in LQC it is a repeller (resp. attractor) in the expanding (resp. contracting) phase. However, whereas in GR the analytical solution is a global attractor in the contracting phase and a repeller in the expanding one, in LQC the others solutions do not catch (do not converge asymptotically) the analytical one because of the bounce, and when they enter in the expanding phase they move away from the analytical orbit depicting at late times a universe with an effective EoS parameter equal to 1 or ∞ .

Acknowledgments

This investigation has been supported in part by MINECO (Spain), projects MTM2014-52402-C3-1-P and MTM2015-69135-P.

-
- [1] A. Einstein, “Die Feldgleichungen der Gravitation,” *Sitzungsberichte der Königlich Preußischen Akademie der Wissenschaften (Berlin)*, Seite 844-847., 1915.
 - [2] L. Fernández-Jambrina and R. Lazkoz, “Equation of state and singularities in FLRW cosmological models,” *J. Phys. Conf. Ser.*, vol. 229, p. 012037, 2010.
 - [3] J. D. Barrow, “Sudden future singularities,” *Class. Quant. Grav.*, vol. 21, pp. L79–L82, 2004.
 - [4] S. Nojiri and S. D. Odintsov, “Quantum escape of sudden future singularity,” *Phys. Lett.*, vol. B595, pp. 1–8, 2004.
 - [5] J. D. Barrow, “More general sudden singularities,” *Class. Quant. Grav.*, vol. 21, pp. 5619–5622, 2004.
 - [6] S. Nojiri, S. D. Odintsov, and S. Tsujikawa, “Properties of singularities in (phantom) dark energy universe,” *Phys. Rev.*, vol. D71, p. 063004, 2005.
 - [7] S. Nojiri, and S. D. Odintsov, “Is the future universe singular: Dark Matter versus modified gravity?,” *Phys. Lett.*, vol. B686, pp. 44–48, 2010.
 - [8] A. V. Astashenok, S. Nojiri, Sergei D. Odintsov, R. J. Scherrer, “Scalar dark energy models mimicking Λ CDM with arbitrary future evolution,” *Phys. Lett.*, vol. B713, pp. 145–153, 2012.
 - [9] M. Bouhmadi-Lopez, P. F. Gonzalez-Diaz, and P. Martin-Moruno, “Worse than a big rip?,” *Phys. Lett.*, vol. B659, pp. 1–5, 2008.
 - [10] S. Nojiri and S. D. Odintsov, “Introduction to modified gravity and gravitational alternative for dark energy,” *eConf*, vol. C0602061, p. 06, 2006. [*Int. J. Geom. Meth. Mod. Phys.* 4,115(2007)].
 - [11] J. de Haro and J. Amorós, “Nonsingular Models of Universes in Teleparallel Theories,” *Phys. Rev. Lett.*, vol. 110, no. 7, p. 071104, 2013.
 - [12] L. Fernández-Jambrina and R. Lazkoz, “Singular fate of the universe in modified theories of gravity,” *Phys. Lett.*, vol. B670, pp. 254–258, 2009.
 - [13] A. A. Starobinsky, “A New Type of Isotropic Cosmological Models Without Singularity,” *Phys. Lett.*, vol. B91, pp. 99–102, 1980.
 - [14] M. V. Fischetti, J. B. Hartle, and B. L. Hu, “Quantum Effects in the Early Universe. 1. Influence of Trace Anomalies on Homogeneous, Isotropic, Classical Geometries,” *Phys. Rev.*, vol. D20, pp. 1757–1771, 1979.
 - [15] E. Elizalde, S. Nojiri, S. D. Odintsov, and S. Ogushi, “Casimir effect in de Sitter and anti-de Sitter brane worlds,” *Phys. Rev.*, vol. D67, p. 063515, 2003.
 - [16] E. Elizalde, S. Nojiri, and S. D. Odintsov, “Late-time cosmology in (phantom) scalar-tensor theory: Dark energy and the cosmic speed-up,” *Phys. Rev.*, vol. D70, p. 043539, 2004.
 - [17] E. Elizalde, S. Nojiri, S. D. Odintsov, and P. Wang, “Dark energy: Vacuum fluctuations, the effective phantom phase, and holography,” *Phys. Rev.*, vol. D71, p. 103504, 2005.
 - [18] L. Amendola, D. Polarski, and S. Tsujikawa, “Are $f(R)$ dark energy models cosmologically viable?,” *Phys. Rev. Lett.*, vol. 98, p. 131302, 2007.
 - [19] S. Nojiri and S. D. Odintsov, “Modified gravity with negative and positive powers of the curvature: Unification of the inflation and of the cosmic acceleration,” *Phys. Rev.*, vol. D68, p. 123512, 2003.
 - [20] K. Bamba, S. Nojiri, and S. D. Odintsov, “The Universe future in modified gravity theories: Approaching the finite-time future singularity,” *JCAP*, vol. 0810, p. 045, 2008.
 - [21] E. Wilson-Ewing, “The Matter Bounce Scenario in Loop Quantum Cosmology,” *JCAP*, vol. 1303, p. 026, 2013.
 - [22] E. Wilson-Ewing, “Ekpyrotic loop quantum cosmology,” *JCAP*, vol. 1308, p. 015, 2013.
 - [23] Y.-F. Cai and E. Wilson-Ewing, “Non-singular bounce scenarios in loop quantum cosmology and the effective field description,” *JCAP*, vol. 1403, p. 026, 2014.
 - [24] J. Haro, “Cosmological perturbations in teleparallel Loop Quantum Cosmology,” *JCAP*, vol. 1311, p. 068, 2013. [Erratum: *JCAP*1405,E01(2014)].
 - [25] J.-L. Lehnert and E. Wilson-Ewing, “Running of the scalar spectral index in bouncing cosmologies,” *JCAP*, vol. 1510, no. 10, p. 038, 2015.
 - [26] E. Elizalde, J. Haro, and S. D. Odintsov, “Quasimatter domination parameters in bouncing cosmologies,” *Phys. Rev.*, vol. D91, no. 6, p. 063522, 2015.
 - [27] J. Haro and E. Elizalde, “Gravitational particle production in bouncing cosmologies,” *JCAP*, vol. 1510, no. 10, p. 028, 2015.
 - [28] J. Quintin, Y.-F. Cai, and R. H. Brandenberger, “Matter creation in a nonsingular bouncing cosmology,” *Phys. Rev.*, vol. D90, no. 6, p. 063507, 2014.
 - [29] S. Hidalgo, “Study of the Singularities in the flat Friedmann-Lemaître-Robertson-Walker Universe,” Master’s thesis, FME (Universitat Politècnica de Catalunya), Barcelona, 2015.
 - [30] K. Bamba, J. de Haro, and S. D. Odintsov, “Future Singularities and Teleparallelism in Loop Quantum Cosmology,” *JCAP*, vol. 1302, p. 008, 2013.
 - [31] R. R. Caldwell, M. Kamionkowski, and N. N. Weinberg, “Phantom energy and cosmic doomsday,” *Phys. Rev. Lett.*, vol. 91, p. 071301, 2003.
 - [32] J. de Haro and J. Amorós, “Viability of the matter bounce scenario in Loop Quantum Cosmology from BICEP2 last data,” *JCAP*, vol. 1408, p. 025, 2014.

- [33] H. Kurki-Suonio, “Cosmology I, University of Helsinki lecture notes,” 2005.
- [34] L. D. Landau and E. M. Lifshitz, “The classical theory of fields,” Course of theoretical physics, vol. 2, 1971.
- [35] P. H. Frampton, K. J. Ludwick, and R. J. Scherrer, “The Little Rip,” Phys. Rev., vol. D84, p. 063003, 2011.
- [36] A. V. Astashenok, S. Nojiri, S. D. Odintsov, and A. V. Yurov, “Phantom Cosmology without Big Rip Singularity”, Phys.Lett., vol. B709, pp. 396-403, 2012.
- [37] L. Fernández-Jambrina, “Grand rip and grand bang/crush cosmological singularities,” Phys. Rev. , vol. D90, p. 064014, 2014.
- [38] S. Watson, “An Exposition on inflationary cosmology,” 2000.
- [39] J. Haro and J. Amorós, “The matter-ekpyrotic bounce scenario in Loop Quantum Cosmology,” In preparation.
- [40] M. Joyce, “Electroweak baryogenesis and the expansion rate of the universe,” Phys. Rev. D, vol. 55, pp. 1875–1878, Feb 1997.
- [41] B. Spokoiny, “Deflationary universe scenario,” Physics Letters B, vol. 315, no. 1, pp. 40 – 45, 1993.
- [42] J. Khoury, B. A. Ovrut, P. J. Steinhardt, and N. Turok, “Ekpyrotic universe: Colliding branes and the origin of the hot big bang,” Phys. Rev. D, vol. 64, p. 123522, Nov 2001.
- [43] P. Singh, “Loop cosmological dynamics and dualities with Randall-Sundrum braneworlds,” Phys. Rev., vol. D73, p. 063508, 2006.
- [44] P. Dzierżak, P. Małkiewicz, and W. Piechocki, “Turning big bang into big bounce. I. Classical dynamics,” Phys. Rev. D, vol. 80, p. 104001, Nov 2009.
- [45] J. Haro and E. Elizalde, “Loop cosmology: Regularization vs. quantization,” EPL (Europhysics Letters), vol. 89, no. 6, p. 69001, 2010.
- [46] Y.-F. Cai, A. Marciano, D.-G. Wang, and E. Wilson-Ewing, “Bouncing cosmologies with dark matter and dark energy,” 2016.